Time-Resolved and Pulsed EPR Studies on the Lowest Excited Triplet State of 1,4-Diphenylbutadiyne

Yasutomo Nagano, Tadaaki Ikoma, Kimio Akiyama, and Shozo Tero-Kubota*

Institute for Chemical Reaction Science, Tohoku University, Sendai 980-8577, Japan

Received: February 24, 1998; In Final Form: April 27, 1998

The short-lived T_1 state of 1,4-diphenylbutadiyne (DPB) has been investigated in various glassy matrices at low temperatures using time-resolved EPR and pulsed EPR methods. Zero-field splitting parameters of $D = -0.250$ cm^{-1} and $E = +0.018$ cm^{-1} were determined. The negative D value was verified from the M_S dependence of the ENDOR frequencies. The hyperfine splitting constants of ring protons were obtained from the electron spin−echo envelope modulation with three-pulse stimulated echo. The spin density distribution on the phenyl groups was estimated from the analysis of the hyperfine splittings at each of the canonical orientations. The moderate spin densities on the phenyl rings indicated that the T_1 state was $^3\pi_x\pi_x^*$ in electronic character. The origin of the large negative D value of DPB has been discussed in terms of the spin−orbit interaction between the close lying $^3\pi_x\pi_x^*$ and $^3\pi_x\pi_y^*$ states.

Introduction

Much attention has been paid to the excited states of diacetylene compounds because the photolysis of their single crystals produces conjugated polymers, which show an excellent nonlinear optical character.[1] It has been reported that the excited triplet states are the key intermediate state in the photoinduced polymerization.[2] However, there have been only a few studies on the electronic structure of the excited triplet states of diacetylenes.

It has been reported that 1,4-diphenylbutadiyne emits phosphorescence ($\nu_{00} = 20\,270$ cm^{-1}) with the lifetime of 0.1 s in an EPA (diethyl ether/isopentane/ethanol, 5:5:2) matrix at −170 °C.[3] Hoshi et al.[4] measured the polarized absorption spectrum in the stretched polyethylene film and assigned their bands on the basis of semiempirical molecular orbital (MO) calculations. Time-resolved (TR) resonance Raman studies suggested that the C≡C symmetric stretching exhibits a low-frequency shift in the lowest excited triplet (T_1) state compared with the ground (S_0) state, indicating that the C≡C bond weakens.[5] Bubeck et al.[6] measured the triplet EPR spectra of biphenylglutarate diacetylene in a single crystal and reported large positive D values of zero-field splitting (ZFS) parameters in several sites: $D = +0.2286, +0.2367, +0.2456$ cm^{-1}. These values are larger than those of dinaphthyldiacetylene and 9,9′-diphenanthryldiacetylene which are deduced from the D^* value.[7] It is, therefore, worthwhile to determine the ZFS parameters and spin density distribution in the T_1 state of the fundamental diacetylene compound.

In the present work, we have studied the T_1 state of 1,4-diphenylbutadiyne (DPB, Figure 1) by using continuous wave time-resolved EPR (CW-TREPR) and pulsed EPR spectroscopies. The molecular axes of *z*, *y*, and *x* are along the triple bonds, perpendicular to the long axis within the molecular plane and normal to the molecular plane, respectively. The unpaired electron spin densities on the phenyl rings were estimated from the analysis of the electron spin−echo envelope modulation (ESEEM) spectra observed by a three-pulse stimulated echo technique. The ZFS parameters as well as its sign were determined: $D = -0.250$ cm^{-1} and $E = +0.018$ cm^{-1}. Despite the unusually large $|D|$ value of DPB, the T_1 state was assigned to be $^3\pi_x\pi_x^*$ in character. The electronic structure has been discussed on the basis of the electron spin distribution and semiempirical MO calculations.

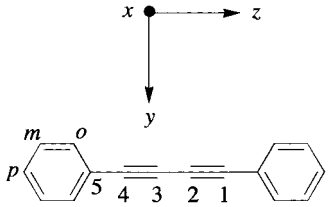

1,4-Diphenylbutadiyne (DPB)

Figure 1. Molecular structure and principal axes of DPB.

Experimental Section

DPB purchased from Aldrich was recrystallized from a mixed solvent of ethanol/acetone (1:1 (v/v)). Spectrograde methylcyclohexane and ethanol were used without further purification. *n*-Butyronitrile was purified by distillation and passing through a basic alumina column followed by dehydration with molecular sieves (4A). Spectrograde toluene was purified by passing through a basic alumina column. The sample solutions of DPB (∼0.01 mol dm^{-3}) were degassed by multiple freeze−pump−thaw cycles. Poly(vinyl alcohol) (PVA) films that incorporated DPB were prepared according to the procedure reported previously.[8]

An excimer laser (Lumonics Hyper EX-400; XeCl, 308 nm) was used as the pulse light source. Magnetophotoselection experiments were performed by passing the laser beam through a Glan laser prism. The CW-TREPR signal was directly detected using an X-band EPR spectrometer (Varian Model E-109E) without field modulation as reported elsewhere.[9] We used a bimodal cavity (Varian E-236), which provides a microwave magnetic field ($\mathbf{B}_1$) parallel to the static magnetic field ($\mathbf{B}_0$) as well as $\mathbf{B}_1 \perp \mathbf{B}_0$. The pulsed EPR measurements were carried out using an X-band pulsed EPR spectrometer (Bruker ESP380E) equipped with a dielectric resonator (Bruker

S1089-5639(98)01274-2 CCC: $15.00
Published on Web 06/19/1998

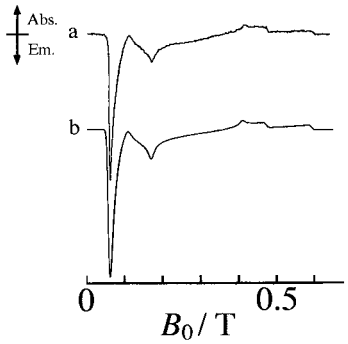

Figure 2. CW-TREPR spectrum of DPB observed 0.3 μs after excitation by pulse laser with 308 nm in a methylcyclohexane glassy matrix at 4 K (a) and its computer simulation (b).

ER4114, $Q \sim 100$). The typical $\pi/2$ pulse width was 16 ns. A three-pulse ($\pi/2-\tau-\pi/2-T-\pi/2$) echo sequence starting from 300 ns after the laser flash was employed to obtain a stimulated echo signal. ESEEM patterns were measured by monitoring echo intensity as a function of the time T between the last two pulses. A helium flow cryostat (Oxford ESR900) was utilized for the measurements at low temperatures.

Results

CW-TREPR. Figure 2a shows the TREPR spectrum of DPB in a methylcyclohexane glassy matrix observed 0.3 μs after a laser flash. The transient EPR signals were clearly observed over the wide range of the magnetic field from about 0.04 to 0.58 T, while the conventional CW-EPR measurements gave only one peak at 0.06 T. The spectral polarity of the $|\Delta M_S| = 1$ transitions is EEE in the low-field region and AAA in the high-field region, where E and A represent enhanced emission and absorption of microwaves, respectively. The polarized EPR signals decayed within 10 μs, though the phosphorescence lifetime was 68 ms in methylcyclohexane at 77 K.

The triplet EPR spectra of the disordered system are interpreted by the spin Hamiltonian comprising electron Zeeman and zero-field interactions:

$$\mathbf{H}_s = g\mu_B\mathbf{B}_0\cdot\mathbf{S} + D_{xx}S_x^2 + D_{yy}S_y^2 + D_{zz}S_z^2$$

$$= g\mu_B\mathbf{B}_0\cdot\mathbf{S} + D(S_z^2 - {}^1/_3\,\mathbf{S}^2) + E(S_x^2 - S_y^2) \qquad (1)$$

The g, μ_B, and $\mathbf{S}$ denote the g factor, the Bohr magneton, and the spin operator for triplet states, respectively. The ZFS parameters of D and E are related to the eigenenergies ($-D_{xx}$, $-D_{yy}$, and $-D_{zz}$) for the T_x, T_y, and T_z sublevels by $D = 3D_{zz}/2$ and $E = (D_{xx} - D_{yy})/2$.

The ZFS parameters of $|D| = 0.250$ cm^{-1} and $|E| = 0.018$ cm^{-1} were determined by computer simulation (Figure 2b). The $|D|$ value obtained is considerably larger than those of diphenylacetylene (0.1426 cm^{-1})[10] and phenylacetylene (0.1339 cm^{-1}).[11] The nonzero E value implies that the two phenyl groups are nearly coplanar in the glassy matrix. If triplet state DPB has two twisted phenyl rings that make 90° of dihedral angle, the E value must be zero because of the S_4 symmetry axis along the z axis.

It should be noted that the strong emissive signal that appeared around 0.06 T does not correspond to the extra canonical, so-called B_{min}. It is due to one of the $|\Delta M_S| = 1$ transitions of the outermost pair. The experimental condition for existence of B_{min} ($|D/\delta| < 3/4$) is not satisfied because of the large D value, where the δ denotes the microwave energy used.[12] We confirmed this fact using a parallel mode cavity, which did not show the typical doublet structure detected at the B_{min} and one of the canonical fields of $|\Delta M_S| = 2$ transitions.

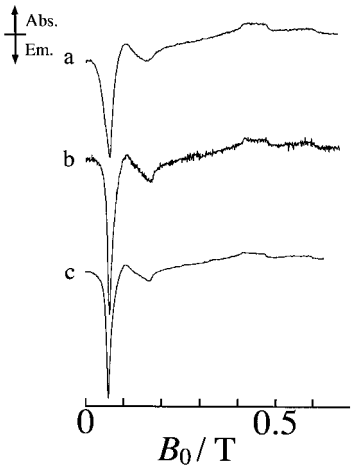

Figure 3. CW-TREPR spectra of DPB observed in the toluene (a), butyronitrile (b), and ethanol (c) glassy matrices at 4 K. The spectra were obtained 0.3 μs after excitation by pulse laser.

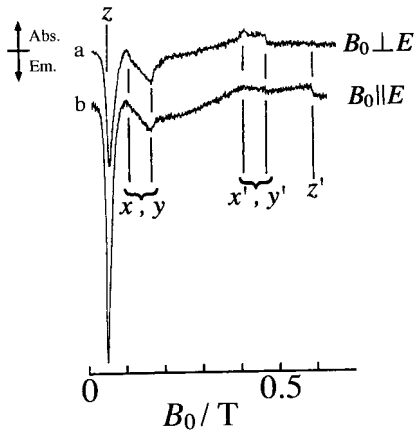

Figure 4. Magnetophotoselection spectra of DPB in a methylcyclohexane glassy matrix at 10 K. The spectra were observed at 0.1 μs after laser pulse excitation with $\mathbf{B}_0\perp\mathbf{E}$ (a) and $\mathbf{B}_0\|\mathbf{E}$ (b).

We observed the matrix dependence of the triplet EPR spectra. Figure 3 shows the TREPR spectra of DPB in three rigid matrices, toluene, *n*-butyronitrle, and ethanol, at 4 K. Although these spectra give the same ZFS parameters, the spectral shape depends on the matrix, indicating that the distributions of the ZFS parameters are different among these systems. In particular, the spectral broadening is significant in the field region lower than 0.06 T. In a toluene glassy matrix, the spectrum shows emissive signals even at zero magnetic field. Similar broadened spectra were observed up to 77 K, suggesting that dynamic effects of molecular motion on the spectral distortion could be neglected. The tailing observed at the lower field of the outermost canonical signal suggests that the inhomogeneous broadening arises from asymmetric distribution of the D value as discussed later.

The magnetophotoselection method is a useful experimental technique for identifying the direction of the principal axes of the ZFS tensor.[13] As shown in Figure 4, the irradiation of DPB with the polarized light gave significant effects on the triplet EPR spectra. When the electric field vector (**E**) of the excitation light was parallel to the $\mathbf{B}_0$, the outermost canonical signals were dominant. On the other hand, the innermost and intermediate pairs became relatively strong in intensity in the case of $\mathbf{E}\perp\mathbf{B}_0$. The UV light with a wavelength of 308 nm excites DPB to the lowest excited singlet (S_1) state. The direction of the $S_1(\pi_x\pi_x^*)$

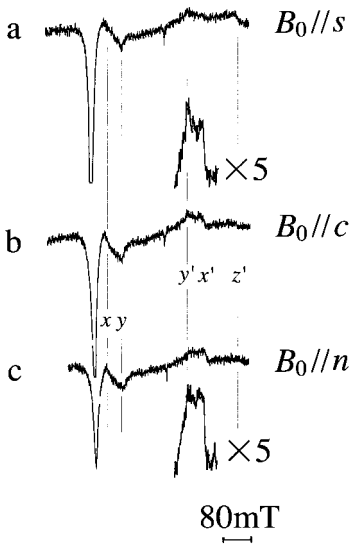

Figure 5. CW-TREPR spectra of DPB measured in a stretched PVA film, where $\mathbf{B}_0$ is parallel to the stretched (*s*) direction (a), in-plane contraction (*c*) direction (b), and normal (*n*) direction of the film plane (c), respectively. The spectra were obtained 0.3 μs after excitation in 77 K.

← S_0 transition moment is along the *z* axis of DPB.[4,14] Thus, we can regard that the signals of the outermost pair correspond to the *z* axis of DPB. The pronounced effect of orientation-selective excitation by the polarized light suggests that the deformation from the linear structure is negligible in the T_1 state of DPB.

To discriminate the out-of-plane *x* axis from the short in-plane *y* axis, we measured the TREPR spectra of partially oriented DPB in a stretched PVA film. Long and planar molecules in the stretched films have a tendency to arrange the long molecular axis along the stretched (*s*) direction and the molecular plane parallel to the film plane.[15−17] As shown in Figure 5a, the alignment of the *z* axis of DPB to the *s* direction was verified by the increase of the outermost canonical signals in $s||\mathbf{B}_0$. It can be expected that the *x* and *y* axes of DPB are along the normal (*n*) direction and the in-plane contraction (*c*) direction of the PVA film, respectively. When the *c* direction was parallel to the $\mathbf{B}_0$, the innermost signals were relatively intensified, as shown in Figure 5b. On the other hand, the intermediate signal became stronger when the *n* direction was parallel to the $\mathbf{B}_0$ (Figure 5c). These orientation effects clearly indicate that the innermost and intermediate canonical signals correspond to those at $\mathbf{B}_0||y$ and at $\mathbf{B}_0||x$, respectively. We can, therefore, describe that the energy order among the spin sublevels is T_z, T_y, and T_x from the top in the case of negative *D* or T_x, T_y, and T_z for positive *D*.

MO Calculations. AM1 RHF-SCF MO calculations for the S_0 and low-lying excited triplet states were carried out by using the MOPAC93 program package.[18] For the configuration interaction calculation of the T_1 state, the two highest occupied (HOMO and HOMO−1) and two lowest unoccupied orbitals (LUMO and LUMO+1) were taken into account. The optimization of the geometry resulted in a planar structure having D_{2h} symmetry in the S_0 and T_1 states. The calculated bond lengths in the S_0 state are $r(C_1{\equiv}C_2)$ = 120 pm and $r(C_2{-}C_3)$ = 135 pm, respectively. These values agree with those determined by X-ray analysis: $r(C_1{\equiv}C_2)$ = 118 pm and $r(C_2{-}C_3)$ = 139 pm, respectively.[19] The calculations indicate that the excitation into the T_1 state induces a stretch of the triple bonds, $r(C_1{\equiv}C_2)$ = 123 pm, and a shortening of the central single bond $r(C_2{-}C_3)$ = 131 pm. The present results agree well with the TR-resonance Raman experiments.[5]

TABLE 1: Spin Density Distribution of DPB in the T_1 State[a]

		C_o	C_m	C_p	C_1	C_2	C_5
expt		0.084 ± 0.016		0.12			
calc[a]	$\pi_x\pi_x^*$	0.069	0.003	0.092	0.149	0.083	0.032
	$\pi_x\pi_y^*$	0.037	0.002	0.046	0.242	0.106	0.018

[a] AM1 calculations were performed with a limited configuration interaction wave functions (MOPAC option CI = 4), taking the two highest occupied and two lowest empty orbitals from the closed-shell SCF calculation into account.

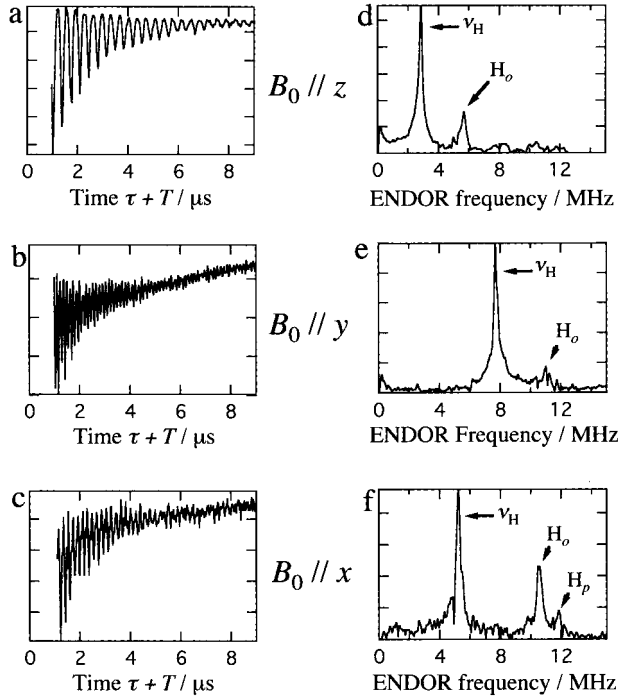

Figure 6. Three-pulse ESE decay envelopes (a−c) and the Fourier transformed spectra (d−f) of DPB in a methylcyclohexane glassy matrix at 4 K. The time intervals between the first two microwave pulses are 176 ns for $\mathbf{B}_0||z$ (66.80 mT), 192 ns for $\mathbf{B}_0||y$ (180.62 mT), and 288 ns for $\mathbf{B}_0||x$ (122.81 mT), respectively.

AM1 calculations indicate that the T_1 state of DPB is ${}^3\pi_x\pi_x^*$ in character in the optimized structure. Table 1 lists the spin densities calculated for the T_1 (${}^3\pi_x\pi_x^*$) as well as the T_3 (${}^3\pi_x\pi_y^*$) states. The spin densities in the phenyl rings decrease in the order of $\rho_p > \rho_o > \rho_m$, and the values are very different in these two states. Thus, the experimental determination of the spin densities is useful in assigning the electronic structure in the T_1 state.

ESEEM Measurements. To observe the hyperfine splittings in the T_1 state of DPB, we measured the three-pulse ESEEM at the stationary fields at 4 K. It has been suggested that the three-pulse ESEEM provides a better spectral resolution than is obtained with the two-pulse method, and the three-pulse sequence further eliminates combination signals of ENDOR frequencies.[20] As shown in Figure 6a−c, the deep modulations were clearly observed at the low-field transitions of each canonical field, while the modulation effects of the higher field transitions were not remarkable. Since the ESEEM arises from simultaneous EPR forbidden transitions as well as allowed ones induced by strong $\mathbf{B}_1$ field, the nuclear modulation effect becomes more prominent at lower $\mathbf{B}_0$ field. In three-pulse ESEEM, the modulation depth with a frequency of ν_a depends on the time interval τ as $\sin^2(\pi\nu_b\tau)$, where ν_a and ν_b are the

ENDOR frequencies in different M_S states connected by the microwave pulse.[21,22] One of the ENDOR frequencies, which is due to the $M_S = 0$ state, is the same as the proton Zeeman frequency (ν_H),[23] because the EPR transitions in the triplet state occur between the $M_S = \pm 1$ and $M_S = 0$ sublevels. Therefore, we optimized the τ value to give the most intense hyperfine lines belonging to the $M_S = \pm 1$ states.[24] The three-pulse ESEEM spectra shown in Figure 6 were observed at proper τ for each canonical fields. After subtraction of a nonoscillating decay by polynomial and the Fourier transformation of the ESEEM spectra, we obtained the corresponding ENDOR frequencies displayed in Figure 6d−f. A few lines appeared at all three stationary fields. We observed very strong signals at 2.84, 7.69, and 5.23 MHz for $\mathbf{B}_0||z$, $\mathbf{B}_0||y$, and $\mathbf{B}_0||x$, respectively. These signals are assigned to the hyperfine line belonging to the $M_S = 0$ sublevel, which is superimposed with the matrix line due to the surrounding methylcyclohexane protons. This was verified by the ESEEM measurements using the duterated methylcyclohexane matrix. Other peaks arise from proton hyperfine splittings in the $M_S = \pm 1$ sublevels.

As shown in Figure 6d, an ESEEM signal was observed at 5.69 MHz, higher frequency than ν_H for $\mathbf{B}_0||z$. We assigned the ENDOR frequency of 5.69 MHz to the ortho-proton (H_o) splitting based on the fact that the signal intensity due to the para-proton (H_p) is expected to be very weak, when $\mathbf{B}_0$ is parallel to the C−H_p bond. Furthermore, the meta-proton (H_m) splitting deduced from the MO calculation is remarkably smaller than the value. For $\mathbf{B}_0||y$, the ESEEM signal was obtained at 11.01 MHz. The signal is also assigned to H_o. The transition probability of the hyperfine signal due to the *p*-proton is expected to be very weak because of the condition of $\mathbf{B}_0 \perp$C−H_p bond. When $\mathbf{B}_0$ is parallel to the *x* axis, $\mathbf{B}_0$ is aligned with the out-of-plane principal axis of the hyperfine tensor, and the echo modulation depth is expected to be small. However, the microwave bandwidth of 16 ns would be wide enough to excite a small fraction of the molecules in which their *x* axes deviate from the $\mathbf{B}_0$ direction around the *x* canonical field.[25] Two hyperfine lines were clearly detected at 10.48 and 11.84 MHz for $\mathbf{B}_0||x$ which were tentatively assigned to H_o and H_p, respectively.

Discussion

Spin Densities and Electronic Character. The semiempirical MO calculation shows that DPB has two nearby triplet states with different characters: $^3\pi_x\pi_x^*$ and $^3\pi_x\pi_y^*$. The former state consists of the two singly occupied out-of-plane π orbitals which are delocalized over a whole molecule, whereas in the latter state the unpaired orbitals are orthogonal to each other in the triple bonds. The electron spin density distribution obtained in the ESEEM experiments would clarify the electronic character of the T_1 state, because the spin densities on the phenyl moieties are significantly different in the $^3\pi_x\pi_x^*$ and $^3\pi_x\pi_y^*$ states, as suggested from the MO calculation (see Table 1).

The ENDOR frequencies observed in the ESEEM spectra can be described by the following effective spin Hamiltonian including the nuclear Zeeman ($\boldsymbol{H}_{nz}$) and hyperfine ($\boldsymbol{H}_{hf}$) interactions:

$$\begin{aligned}\mathbf{H} &= \mathbf{H}_s + \mathbf{H}_{nz} + \mathbf{H}_{hf} \\ &= \mathbf{H}_s - g_H\mu_H\mathbf{B}_0\cdot\mathbf{I}_H + \mathbf{S}\cdot\mathbf{A}_H\cdot\mathbf{I}_H \qquad (2)\end{aligned}$$

where the unpaired electrons interact with a single proton ($I = {}^1/_2$). The notations have their usual meaning. Figure 7 depicts

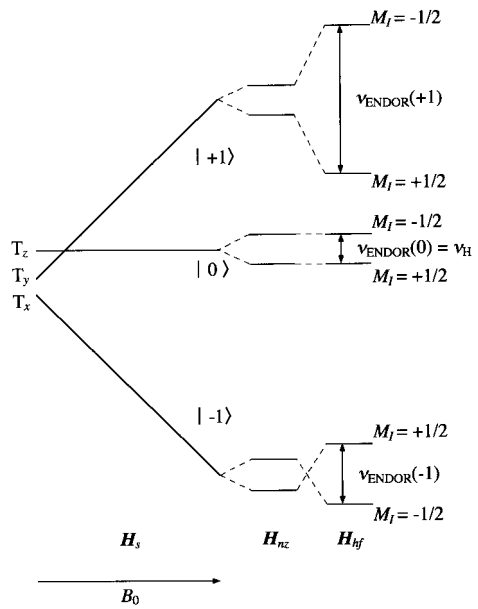

Figure 7. Energy level scheme in the case of $\mathbf{B}_0||z$ with $D < 0$ and the first-order hyperfine interaction with one proton for $A_{zz} < 0$. To describe concisely the case of $\mathbf{H}_{nz} < \mathbf{H}_{hf}$ was drawn, but it is the same as the general case qualitatively.

a typical energy scheme. According to the first-order perturbation of electron spin states, the analytic solution for ENDOR frequencies in triplet state is given by

$$\nu_{ENDOR}(M_S) = [M_s^2\mathbf{h}^T\cdot\mathbf{A}_H^2\cdot\mathbf{h} - 2M_s g_H\mu_H B_0\mathbf{h}^T\cdot\mathbf{A}_H\cdot\mathbf{h} + (-g_H\mu_H B_0)^2]^{1/2} \quad (3)$$

where $\mathbf{h}$ represents the direction cosine of the $\mathbf{B}_0$ for the hyperfine principal axis system.[26,27] Superscript T means the transpose. This expression clearly states that the ENDOR frequency depends on the quantum number of electron spin state as illustrated in Figure 7.

The proton hyperfine tensor of $\mathbf{A}_H$ consists of the isotropic and anisotropic components. In the case of the α proton, the isotropic Fermi contact interaction is induced by a spin exchange mechanism. Using the McConnell relation ($A^{iso} = Q_H\rho$), the splitting constant can be related to the π-spin density ρ at the carbon site where the proton is bonded. The anisotropic part (A^{aniso}) of $\mathbf{A}_H$ originates in the dipolar interaction between electron and nuclear spins, which is also nearly proportional to the spin density on the nearest carbon. The electron spin densities on the phenyl rings were estimated by using the hyperfine principal values for the triplet state of benzene: $Q = -72.5$ MHz, $A_{||C-H} = +35.04$ MHz, $A_{\perp C-H} = -40.36$ MHz, and $A_\perp = +5.31$ MHz.[28] The reduction of hyperfine splitting induced by the mixing between $M_S = \pm 1$ states due to zero-field interaction was also taken into account in calculating the spin density.[29]

By using eq 3, the electron spin densities for the ortho-proton were estimated as $\rho_o = 0.082$, 0.069, and 0.10 from the signals (ENDOR frequency: 5.69, 11.01, 10.48 MHz) observed in three canonical orientations. The variation in three orientations may arise from the neglect of the dipolar interactions between the proton and the electron spins on the nonadjacent carbons. The average value of $\rho_o = 0.084$ was obtained for the electron spin density at the ortho-position. The spin density at the para-position of $\rho_p = 0.12$ was also estimated from the 11.84 MHz at $\mathbf{B}_0||x$, as listed in Table 1. The electron spin densities indicate that the T_1 state of DPB is $^3\pi_x\pi_x^*$ in character like phenylacety-

lene[11] and diphenylacetylene[10] despite its unusually large $|D|$ value. About 30% of unpaired electrons stays in each phenyl ring and the rest, 40%, exists in the triple bond part.

Sign of the ZFS Parameters. Since the intersystem crossing (ISC) process in DPB remains obscure, we could not determine unequivocally the sign of the ZFS parameters from the polarization pattern of the TREPR spectra. ESEEM spectra provide information about the sign of the ZFS parametrs. It should be noted that the sign of the D value can be determined from the ESEEM pattern on the basis of the following general facts:

(1) All diagonal elements in the hyperfine splitting tensor due to the α-proton are negative due to the large negative isotropic elements Q.

(2) In the $|+1\rangle$ state, the $M_I = -1/2$ and $+1/2$ states are, therefore, destabilized and stabilized by the hyperfine interaction, respectively. In contrast, the hyperfine interaction causes the opposite energy shifts of these nuclear spin states in the $|-1\rangle$ state (Figure 7). The splitting of $\nu_{ENDOR}(0)$ in the $|0\rangle$ state corresponds to the free proton frequency (ν_H).

(3) Thus, the hyperfine line of $\nu_{ENDOR}(+1)$ in the ESEEM spectrum observed in the $|+1\rangle \leftrightarrow |0\rangle$ EPR transition should appear at the higher frequency compared with ν_H. On the other hand, the $|-1\rangle \leftrightarrow |0\rangle$ EPR transition should give the hyperfine signal of $\nu_{ENDOR}(-1)$ at the lower frequency region than ν_H in the condition of $|\mathbf{h}^T\cdot\mathbf{A}_H^2\cdot\mathbf{h}/\ \mathbf{h}^T\cdot\mathbf{A}_H\cdot\mathbf{h}| < 2\nu_H$ or at the higher frequency region in the $|\mathbf{h}^T\cdot\mathbf{A}_H^2\cdot\mathbf{h}/\mathbf{h}^T\cdot\mathbf{A}_H\cdot\mathbf{h}| > 2\nu_H$ condition.

In the case of negative D ($T_z > 0 > T_y > T_x$, here $E > 0$), the EPR transitions of low-field sides for $\mathbf{B}_0||z$, $\mathbf{B}_0||y$, and $\mathbf{B}_0||x$ correspond to $|-1\rangle \leftrightarrow |0\rangle$, $|+1\rangle \leftrightarrow |0\rangle$, and $|+1\rangle \leftrightarrow |0\rangle$, respectively.[30] In contrast, if D is positive ($T_x > T_y > 0 > T_z$, here $E < 0$), the transitions for $\mathbf{B}_0||z$, $\mathbf{B}_0||y$, and $\mathbf{B}_0||x$ are $|+1\rangle \leftrightarrow |0\rangle$, $|-1\rangle \leftrightarrow |0\rangle$, and $|-1\rangle \leftrightarrow |0\rangle$, respectively.

All ESEEM signals were observed at a higher frequency region compared with ν_H for three canonical fields in the present system. Assignment of the ENDOR frequencies to give the reasonable spin density on the ortho-proton suggests that $|\mathbf{h}^T\cdot\mathbf{A}_H^2\cdot\mathbf{h}/\mathbf{h}^T\cdot\mathbf{A}_H\cdot\mathbf{h}| > 2\nu_H$ for $\mathbf{B}_0||z$, while $|\mathbf{h}^T\cdot\mathbf{A}_H^2\cdot\mathbf{h}/\mathbf{h}^T\cdot\mathbf{A}_H\cdot\mathbf{h}| < 2\nu_H$ for $\mathbf{B}_0||y$ and $\mathbf{B}_0||x$. The results prove that the low-field EPR transition for $\boldsymbol{B}_0||z$ corresponds to that of $|-1\rangle \leftrightarrow |0\rangle$, whereas they are the transition of $|+1\rangle \leftrightarrow |0\rangle$ for $\mathbf{B}_0||y$ and $\mathbf{B}_0||x$. Therefore, we conclude that the sign of the D value is negative in the T_1 state of DPB.

Despite the relatively large distribution of spin density in the T_1 state of DPB, the $|D|$ value of 0.25 cm^{-1} is much larger than those of phenylacetylene and diphenylacetylene.[10,11] The D value of hydrocarbon compounds is well-known to be governed by the electron spin dipole−dipole interaction because of the small spin−orbit coupling (SOC) constant of the carbon atom ($\lambda_C = 32$ cm^{-1}).[31−33] However, the electron spin dipole−dipole interaction is unable to give such a large $|D|$ value in the $^3\pi_x\pi_x^*$ state. ZFS parameters due to the spin dipole−dipole interaction were calculated using semiempirical SCF π-electron molecular orbital theory.[34] Wave functions were constructed from Pariser−Parr−Pople type LCAO MOs by including configurations arising from the main single excitations relative to the ground state. The spin dipole−dipole interactions were calculated using double-ζ atomic orbitals by Clementi.[35] The geometry of DPB was taken from the optimization result by the AM1 RHF−SCF MO method. The calculations gave the ZFS parameters of $D = -0.114$ cm^{-1} and $E = -0.0046$ cm^{-1}. The $|D|$ value calculated is less than half of the present experimental result. Therefore, the SOC should contribute to the ZFS splitting, suggesting the very small energy difference between $^3\pi_x\pi_x^*$ and $^3\pi_x\pi_y^*$. The SOC effect on the D value of ZFS parameters is expressed by

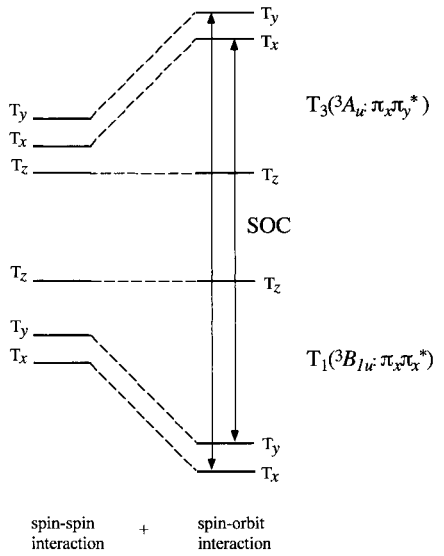

Figure 8. Schematic energy diagram for the triplet sublevels of DPB.

$$D^{SOC} = \frac{3}{2}D_{zz}^{SOC} = -\lambda_C{}^2\frac{|\langle{}^3\pi_x\pi_x^*|\sum_{k=1}^{4} l_z^k|{}^3\pi_x\pi_y^*\rangle|^2}{\Delta\epsilon({}^3\pi_x\pi_y^* - {}^3\pi_x\pi_x^*)} \quad (4)$$

Here, only the z element (l_z^k) in orbital angular momentum of the kth carbon can operate efficiently at the one-centered integrals in numerator. Figure 8 shows the schematic energy diagram of the $^3\pi_x\pi_x^*$ and $^3\pi_x\pi_y^*$ states in adding SOC of eq 4. The negative large D value in the $^3\pi_x\pi_x^*$ of DPB is well-explained by the SOC with the close-lying $^3\pi_x\pi_y^*$. We can reproduce the observed D value by the SOC with the energy difference ($\Delta\epsilon$) of ca. 1000 cm^{-1} between these two states. Polyyne type molecules have the orthogonal π orbitals on the same carbon, leading to different behavior from polyene type molecules in the excited states. This characteristic can make the SOC contribution to ZFS parameters effectively even at the carbon center. Despite no experimental evidence, the positive D value was reported for the related molecule of biphenylglutarate diacetylene in a single crystal.[6] According to the present result, the D value of biphenylglutarate diacetylene is speculated to be negative unless a drastic structural change is induced by the substituent group.

Matrix Dependence of the TREPR Spectra. The TREPR spectrum of DPB observed in a methylcyclohexane glassy matrix was well-reproduced by using the Gaussian type line shape with a half-width at half-height of 5 mT (see Figure 2). However, we obtained poor fits in the simulation for the TREPR spectra in toluene, *n*-butyronitrile, and ethanol despite the complete coincidence of the canonical fields in these spectra. In particularly, there are large residuals in the fits in the field region lower than 0.06 T. The inhomogeneous broadening may arise from the asymmetric distribution of the ZFS parameters. Environmental effects could induce the relatively small variations for the twisting angle of the phenyl groups in DPB, as reported in carbonyl molecules[36−38] in solid matrices. The energy gap, $\Delta\epsilon(^3\pi_x\pi_y^* - {}^3\pi_x\pi_x^*)$, decreases with the increasing of the twist angle resulting in the increase of the $|D^{SOC}|$ value. In the soft matrix such as methylcyclohexane, the molecular conformational heterogeneity is considered to be small and DPB keeps the planar conformation.

Intersystem Crossing. From the polarity of the TREPR spectrum and the negative D value, it was elucidated that the ISC occurs preferentially into the T_z sublevel of the T_1 state from the S_1 state. It has been assigned that the S_1 state of DPB is $\pi_x\pi_x^*$ ($^1B_{1u}$).[4] Because direct SOC between the $S_1(B_{1u})$ and $T_1(B_{1u})$ states is impossible, some vibronic spin−orbit coupling must be considered for the ISC process. Preferential ISC would occur from the S_1 state to the T_z sublevel (B_{1u}) of the $^3\pi_x\pi_y^*$ (^3A_u) state following the internal conversion promoted by the vibrational modes with b_{1g} symmetry. The spin polarization in the T_z sublevel is kept through the internal conversion route from the $^3\pi_x\pi_y^*$ state to the T_1 state.

Conclusion

A very large $|D|$ value of ZFS parameters was observed in the T_1 state of DPB using the CW-TREPR technique. The principal axes of the fine structure tensor were identified by the magnetophotoselection experiment and by utilizing stretched PVA films, suggesting that a linear planar structure was retained in the T_1 state. The ESEEM signals on the T_1 state of DPB were observed even in a glassy matrix using three-pulse sequences. The spin densities on the ortho and para carbons of phenyl groups were estimated. The moderate spin densities on the phenyl rings indicate that the electronic configuration of the T_1 state is $^3\pi_x\pi_x^*$ in character. On the basis of the negative large D value, we conclude that the spin−orbit interaction with the close lying $^3\pi_x\pi_y^*$ state governs the ZFS parameters.

Acknowledgment. We are grateful to Prof. M. Yagi and Mr. M. Noda, Yokohama National University, for their help in preparing stretched PVA films. We also thank Prof. J. Higuchi and Prof. S. Yamauchi for their helpful discussion. The present research was supported in part by a Grant-in-Aid of Scientific Research No. 07404040 from the Ministry of Education, Science, Sports and Culture, Japan.

References and Notes

(1) Chemla, D. S., Zyss, J., Eds. *Nonlinear Optical Properties of Organic Molecules and Crystals*; Academic Press: Orlando, FL, 1987; Vol. 2.

(2) Sixl, H. In *Advances in Polymer Science*; Cantow, H.-J., Ed.; Springer-Verlag: Berlin, Heidelberg, 1984; Vol. 63, p 49.

(3) Beer, M. *J. Chem. Phys.* **1956**, *25*, 745.

(4) Hoshi, T.; Okubo, J.; Kobayashi, M.; Tanizaki, Y. *J. Am. Chem. Soc.* **1986**, *108*, 3867.

(5) Yoneda, H.; Hiura, H.; Takahashi, H. *J. Mol. Struct.* **1993**, *301*, 47.

(6) Bubeck, C.; Sixl, H.; Bloor, D.; Wegner, G. *Chem. Phys. Lett.* **1979**, *63*, 574.

(7) Webber, S. E.; Wade, C. G. *J. Chem. Phys.* **1972**, *57*, 2219.

(8) Yagi, M.; Shioya, Y.; Higuchi, J. *J. Photochem. Photobiol. A: Chem.* **1991**, *62*, 65.

(9) Ikoma, T.; Akiyama, K.; Tero-Kubota, S.; Ikegami, Y. *J. Phys. Chem.* **1989**, *93*, 7087.

(10) Higuchi, J.; Ito, T.; Kanehisa, O. *Chem. Phys. Lett.* **1973**, *23*, 440.

(11) Hirota, N.; Wong, T. C.; Harrigan, E. T. *Mol. Phys.* **1975**, *29*, 903.

(12) de Groot, M. S.; van der Waals, J. H. *Mol. Phys.* **1960**, *3*, 190. The nonzero E value does not influence the condition under which B_{min} exists if $|D| \geq 3|E|$ is satisfied.

(13) Ikoma, T.; Akiyama, K.; Tero-Kubota, S.; Ikegami, Y. *J. Phys. Chem.* **1991**, *95*, 7119.

(14) Thulstrup, E. W.; Michl, J. *J. Am. Chem. Soc.* **1982**, *104*, 5594.

(15) Ito, T.; Higuchi, J.; Hoshi, T. *Chem. Phys. Lett.* **1975**, *35*, 141.

(16) Higuchi, J.; Ito, T.; Yagi, M.; Minagawa, M.; Bunden, M. *Chem. Phys. Lett.* **1977**, *46*, 477.

(17) Yagi, M.; Uchida, K.; Higuchi, J. *Chem. Phys. Lett.* **1984**, *108*, 111.

(18) Dewar, M. J. S.; Zoebisch, E. G.; Healy, E. F.; Stewart, J. J. P. *J. Am. Chem. Soc.* **1985**, *107*, 3902.

(19) Wiebenga, E. H. *Z. Kristallogr*. **1940**, *102*, 193.

(20) Lin, T.-S. *Chem. Rev.* **1984**, *84*, 1.

(21) Atherton, N. M. *Principle of Electron Spin Resonance*; Ellis Horwood: Chichester, England, 1993; Chapter 11.

(22) Dikanov, S. A.; Tsvetkov, Y. D. *Electron Spin−Echo Envelope Modulation Spectroscopy*; CRC Press: Boca Raton, FL, 1992.

(23) $\nu_n = g_n\mu_nB_0/h$, where g_n and μ_n denote the nuclear g factor and magneton, respectively.

(24) The hyperfine line owing to the $M_S = \pm 1$ state reaches a maximum for $\tau = (2m + 1)/2\nu_H$, $m = 0, 1, 2$, etc.

(25) Seidel, H.; Mehring, M.; Stehlik, D. *J. Chem. Phys.* **1985**, *83*, 956.

(26) Chapter 5, Section 5.2 in ref 21.

(27) Weil, J. A.; Bolton, J. R.; Wertz, J. E. *Electron Paramagnetic Resonance*; Wiley: New York, 1994; Chapter 5, Section 5.3.

(28) Clarke, R. H.; Hutchison, C. A., Jr. *J. Chem. Phys.* **1971**, *54*, 2962.

(29) Ohba, Y.; Kawata, S.; Satoh, M.; Yokoi, H.; Iwaizumi, M. In *Electron Magnetic Resonance of Disordered Systems*; Yordanov, N. D., Ed.; World Scientific: Singapore, 1991; p 175. At one of the canonical fields, B_i, the spin functions for the highest ($|+\rangle$) and lowest ($|-\rangle$) sublevels are expanded by the spin functions under infinite field such as $|+\rangle = \cos\theta_i|+1\rangle + \sin\theta_i|-1\rangle$, $|-\rangle = -\sin\theta_i|+1\rangle + \cos\theta_i|-1\rangle$, and $\tan 2\theta_i = (D_{jj} - D_{kk})/2g\mu_BB_0$.

(30) The quantum numbers for the electron spin state under infinite field are good enough to interpret the sign of the D value qualitatively.

(31) McGlynn, S. P.; Azumi, T.; Kinoshita, M. *Molecular Spectroscopy of The Triplet State*; Prentice Hall: Englewood Cliffs, NJ, 1969; Chapter 9, Section 3.

(32) Chapter 6, section 6.4, in ref 21.

(33) Murov, S. L., Carmichael, I., Hug, G. L., Eds. *Handbook of Photochemistry*; Dekker: New York, 1993; Chapter 16.

(34) Higuchi, J. *Bull. Chem. Soc. Jpn.* **1981**, *54*, 2864.

(35) Clementi, E. Tables of Atomic Functions. *IBM J. Res. Dev.* **1965**, *9*, 2 (Supplement, Tables 45-01).

(36) Horie, K.; Morishita, K.; Mita, I. *Macromolecules* **1984**, *17*, 1746.

(37) Hochstrasser, R. M.; Wessel, J. E. *Chem. Phys. Lett.* **1973**, *19*, 156.

(38) Lipson, M.; McGarry, P. F.; Koptyug, I. V.; Staab, H. A.; Turro, N. J.; Doetschman, D. C. *J. Phys. Chem.* **1994**, *98*, 7504.